Effect of photodetachment on a radio-frequency discharge through BCl_3

Carl E. Gaebe, Todd R. Hayes, and Richard A. Gottscho
AT&T Bell Laboratories, Murray Hill, New Jersey 07974-2070
(Received 29 August 1986)

We present a novel spectroscopic diagnostic that provides a detailed picture of a radio-frequency discharge's response to photodetachment of electrons from negative ions. Spatially and temporally resolved changes in the local electric field of a 50-kHz discharge through BCl_3 are monitored using Stark-mixing spectroscopy. These local measurements are also compared to current transients that appear simultaneously in the external circuit (optogalvanic effect). Both the external current and the local field exhibit oscillations at frequencies characteristic of ion motion; however, the local measurements provide a more detailed picture of the changes in sheath structure. Near the momentary anode, the sudden increase in negative charge mobility causes a reduction in the sheath field magnitude but an overall increase in sheath thickness. Initially, the plasma potential floats up toward the anode potential because of the loss of negative charge but subsequently decreases below the initial level as the system relaxes back to steady state in an oscillatory manner.

I. INTRODUCTION

Photodetachment of electrons from negative ions in dc discharges has been used recently for determining the number density of negative ions and for determining the electron affinities of various atoms and molecules.[1-7] The sudden change in electron density resulting from photodetachment has been detected using microwave interferometry,[1,7] Langmuir probes,[2,3,7] and optogalvanic spectroscopy.[4-7] While the first two methods can give an unambiguous measure of the initial negative ion density, the third measures the change in the discharge current that results from the increased mobility of electrons relative to negative ions and as such is not a readily definable function of the initial negative ion density.

The optogalvanic effect produced by photodetachment of electrons from negative ions is complicated by the interactions between electrons, ions, and the local electric field. For example, in weakly ionized plasmas the creation of electrons from negative ions leads to a decrease in the local field as the plasma becomes more conducting. However, as the field decreases, the attachment rate may increase and electrons may convert back into negative ions causing the field to increase once more. In general, optogalvanic signals generated by processes other than photodetachment produce a similar, complicated plasma response. Because of the complexity of optogalvanic mechanisms, the effect has been used only sparingly as a quantitative tool. A more detailed description of the plasma response is needed both to provide a basis for using the optogalvanic signal quantitatively and to generate insight into the kinetic balance responsible for sustaining the discharge.

In this work, we present a novel pump and probe spectroscopic diagnostic that provides a detailed picture of the plasma response to photodetachment. In a time- and space-resolved manner, we employ the nonintrusive technique of Stark-mixing spectroscopy[8-10] to monitor changes in the local electric field which result from photodetachment of electrons from negative ions. The field is integrated to obtain the plasma potential and is differentiated to obtain the net charge distribution. The experiments are performed in the electrode sheath region of a 50-kHz rf discharge through BCl_3 at a time in the cycle when the negative ion density is a maximum.[11,12]

Radio frequency discharges through BCl_3 are chosen for study for several reasons: (1) the presence of BCl radicals permits the use of Stark-mixing spectroscopy to determine the local electric field magnitude with fair sensitivity (~ 75 V/cm);[9] (2) the conditions required for producing large numbers of negative ions have been determined previously;[11] and (3) BCl_3 rf discharges are used in the etching of thin films in microelectronic device fabrication[13-18] and better understanding of attaching gas discharge physics may improve manufacturing process control.

In Sec. II, we describe the experimental apparatus, for which additional details can be found elsewhere.[19-22] In Sec. III A, the optogalvanic signal resulting from photodetachment of electrons from negative ions in a BCl_3 discharge is described. In Sec. III B, the effects of photodetachment on the local electric field, plasma potential, and charge density are presented and compared to the optogalvanic signal. In Sec. IV, the major results of this work and implications for further studies are summarized.

II. EXPERIMENTAL

A schematic diagram of the apparatus is presented in Fig. 1. A 50-kHz, 10-W discharge is maintained between a pair of fiat stainless steel electrode plates measuring 7.62 cm in diameter and spaced 1.6 cm apart. BCl_3 continuously flows through the discharge cell at a rate of 10 sccm (4×10^{-4} mole/min) and is maintained at a pressure of 300 mTorr. Typical plasma parameters are estimated to be the following: charge density $\sim 10^{11}$ cm^{-3}, average electron energy ~ 2 eV, fractional ionization $\sim 10^{-5}$, and Debye length $\sim 30\ \mu$m.

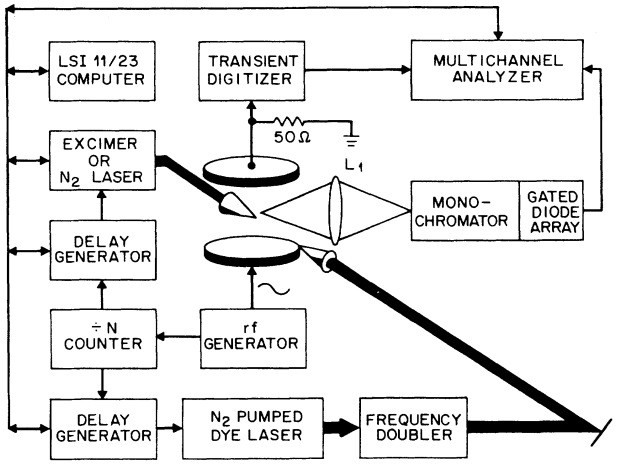

FIG. 1. Schematic diagram of the experimental setup. Negative ions formed in an rf discharge are photodetached using either an excimer or a nitrogen laser. The resulting optogalvanic signals are detected using a transient recorder or, alternatively, by monitoring changes in the Stark-affected LIF spectra of BCl radicals near the photodetachment region.

A. Optogalvanic detection

To photodetach electrons, an excimer ($\lambda=308$ nm) [or a nitrogen ($\lambda=337$ nm)] laser is triggered synchronously with the applied rf field[21] and the beam is passed through the reactor near the upper electrode, which is connected to ground potential through a 50 ohm resistor. The voltage across this resistor is measured using a fast transient digitizer (Biomation model 8100). For background acquisition, a shutter (not shown) is used to block passage of the detaching laser beam through the cell. With the shutter closed, the digitizer records only the steady-state waveform resulting from the rf current through the discharge. With the shutter open, both the optogalvanic and steady-state signals are recorded. By subtracting an equal number of "laser off" waveforms from "laser on" waveforms the fully time-resolved optogalvanic transient is recovered.[11] It should be noted that this method of recovering the optogalvanic waveform from an rf discharge differs from previous methods which rely upon phase-sensitive detection.[23–25] Thus, the optogalvanic signal is characterized by more than just an amplitude and phase shift and detailed comparison with theory is possible.

The ultimate sensitivity of this method is limited by the shot noise in the instantaneous rf current. For a discharge current of 60 mA, a detection bandwidth of 50 MHz, and a signal/noise ratio of 2:1 the shot-noise limit is estimated to be $\sim 2\times 10^4$ photodetached electrons. In practice, we observe that discharge current instabilities limit the sensitivity to only $\sim 10^7$ photodetached electrons. For an interaction volume of 0.1 cm^3, this corresponds to an anion density of $\sim 10^8$ cm^{-3}.

B. Local field measurements

The local electric field is measured *in situ* and nonintrusively by spectrally resolving laser-induced fluorescence (LIF) from Stark-mixed parity levels of BCl radicals produced by the discharge.[8,9] The frequency-doubled output beam of a N_2-pumped dye laser excites a particular rovi- bronic level of the $A\ ^1\Pi$ state of the BCl radical ($\lambda\approx$ 272 nm). Either the $P(6)$ or the $P(12)$ rotational lines are used, depending on the magnitude of the field to be measured.[9]

The intersection of the field of view of the fluorescence collection optics and the dye laser beam determines the region of the plasma where the field is measured. Typically, this region is $\sim$ 100 μm along the electric field axis (i.e., normal to the electrode surfaces) and 1 cm along the radial direction. The distance from the electrode surface is determined by measuring the plasma-induced emission axial profile as described previously.[20] The position of the photodetachment laser beam relative to the field-probe beam is determined to better than 50 μm by filling the cell with an atmosphere of nitrogen and scanning the fluorescence collection optics to measure the Rayleigh scattering profile. From this profile a full width at half maximum (FWHM) intensity of 1 mm is determined along the electric field axis. In the radial direction, the FWHM is approximately 3 mm.

The response of the plasma field to the photodetachment pulse is mapped out in time and space by one of the following two methods: (1) fixing the spatial separation between the two beams and scanning the time delay; or (2) fixing the time delay between the two laser pulses and scanning the probe laser beam position for a fixed photodetachment laser beam position.

III. RESULTS AND DISCUSSION

In this section, we first discuss the optogalvanic signal and then the *in situ* field measurements which provide more detailed information on the effect that photodetachment has on the plasma. Except where noted, the photodetaching laser beam is positioned 2 mm from the grounded electrode, near the plasma-sheath boundary (Fig. 2). The detaching laser is always fired at times in the cycle when the nearby, grounded electrode is the momentary anode.

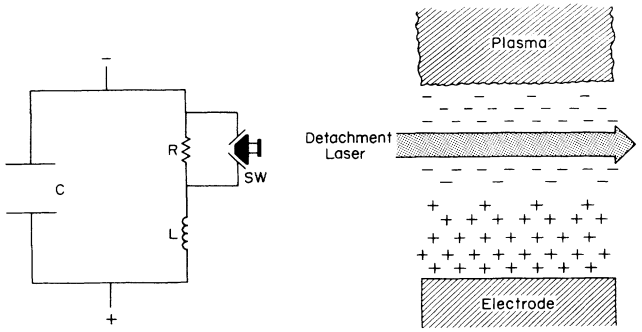

FIG. 2. Schematic illustration of the photodetachment experiment and equivalent circuit analogue. Electrons are detached from negative ions at a position of 2 mm from the momentary anode. A charge double layer exists prior to photodetachment. The sheath properties are represented by a series resistor (R) and inductor (L) in parallel with a capacitor (C). The photodetachment laser pulse is represented by depression of a momentary switch (SW) which short circuits the sheath resistance.

A. Photodetachment-optogalvanic signal

Two cycles of a typical rf current waveform, with the photodetachment current transient superimposed, are shown in Fig. 3(a). Electrons from what is presumed to be BCl_3^- (Ref. 11) are detached using a N_2 laser at 337.1 nm. The photodetaching laser beam is positioned one mm from the upper, grounded electrode and triggered at a time (dashed line in Fig. 3) in the rf cycle corresponding to $\omega t = 0.2\pi$ ($\omega t = 0$ is defined to occur when the voltage on the upper electrode relative to the lower electrode changes from negative to positive). Figure 3(b) shows just the photodetachment-induced current obtained after subtraction of the background rf current. We have shown previously[11] that as a result of rapid electron energy relaxation and subsequent attachment, the negative ion density reaches a maximum at this time in the cycle.

The transients in Fig. 3(b) do not lend themselves to simple interpretation despite the high time resolution with which they have been recorded. The initial optogalvanic signal at 0.2π includes current from the nascent detached electrons. Subsequent oscillations occur at a frequency of 6—7 MHz,[11] which is characteristic of ion motion, but the origin of these oscillations is not obvious. The remaining signals near 1.2π, 2.4π, and 3.2π [Fig. 3(b)] are associated with cusp-like features in the rf current [Fig. 3(a)], which are believed to result from the sudden extraction of positive and negative ions from the sheaths when the local field reaches a critical amplitude.[11,21] The persistence of the optogalvanic signal over several cycles is indicative of the time scale for the return to steady state and is a function of ionization, diffusion, and secondary emission processes. Kramer[26] has made similar observations upon photodetachment of electrons from Cl^- in 13.56 MHz discharges through Cl_2. Preliminary results from a fluid model description of discharges operated at 50 kHz (Refs. 27 and 28) as well as kinetic modeling of higher frequency discharges through Cl_2 (Ref. 29) also indicate that several 50 kHz cycles are necessary for re-establishment of steady state.

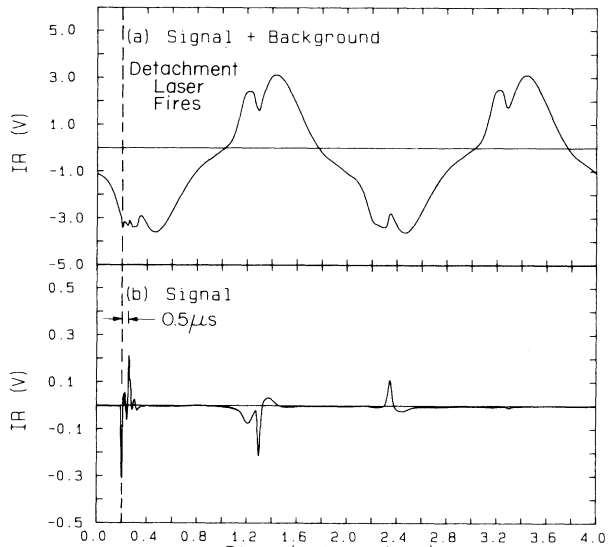

FIG. 3. *Ex situ* optogalvanic signal produced by photodetachment of BCl_3^- ions. (a) A 1000 shot average as it appears before background subtraction. (b) The same signal after subtracting 1000 background shots. Time in units of π refers to the phase of the voltage on the upper (grounded) electrode relative to the lower (powered) electrode (see text). The laser fires at $\omega t = 0.2\pi$, as indicated by the arrow and dashed line. The time scale of 0.5 μs is indicated for the *in situ* field probe measurements in Fig. 4.

B. Local plasma response

In order to gain further insight into the effects caused by photodetachment, it is advantageous to measure changes in the local electric field. First, the temporal variation in the field at several fixed spatial separations of the two laser beams is examined. Second, the spatial variation for several fixed time delays is examined. The plasma potential and net charge density are determined directly by integrating and differentiating the measured field, respectively. Finally, the space-time field, potential, and charge density are displayed as color contour plots to convey a better qualitative feeling for the response of the discharge to the photodetaching laser pulse.

1. Temporal variation of the field at several spatial separations

In this section, we examine the temporal dependence of the local field at several positions for 0.5 μs after the photodetachment laser pulse. The time scale for which local field measurements are made is indicated in Fig. 3(b).[12]

The detachment laser is fired at various times before the probe laser[30] and is positioned 2 mm below the upper electrode near the plasma-sheath boundary where the optogalvanic signal is observed to be largest. The probe laser beam is fired at $\omega t = 0.2\pi$ and is positioned 2.5, 2.0, 1.5, and 1.0 mm from the electrode (momentary anode). The results are shown in Fig. 4 along with a schematic representation of the detaching and probing laser beam positions in the sheath. Several features are noteworthy.

(1) Because of the large negative ion density, the plasma potential initially lies below the anode potential by 120 V and the field exhibits a maximum of 600 V/cm at a position of 1.5 mm from the electrode.[11] A maximum in the electric field implies the existence of a charge double layer and capacitive energy storage (Fig. 2).[31—33]

(2) [See Fig. 4(a).] The field just inside the plasma body (2.5 mm) is initially below our detection limit (75 V/cm). On liberating electrons at 2.0 mm, the field at 2.5 mm increases rapidly and then relaxes monotonically back to its original level. This initial increase in the field represents an expansion of the sheath as a result of the increase in positive space charge left behind when electrons are accelerated toward the momentary anode (see also Figs. 5—7).

(2) In the sheath [Figs. 4(b)—4(d)], the field initially decreases in a time comparable to or shorter than our time resolution (~20 ns); relaxation back to the initial condition is oscillatory, not monotonic. The absence of a

detectable delay between photodetachment and onset of the field change is consistent with known electron drift velocities at the initial field of ~ 600 V/cm.[34] The initial decrease in the field near the anode is consistent with the sheath becoming more conducting as a result of the increase in negative charge mobility. An analogous situation would be the momentary short circuiting of a resistor in parallel with a capacitor: the current momentarily increases as the stored charge (in the double layer) is dissipated and the voltage decreases (Fig. 2).

(3) The field oscillations observed in the region between the detachment laser and the momentary anode occur at nearly the same frequency as the current oscillations detected in the external circuit (6–7 MHz) [see Fig. 3 above and Fig. 3(a) in Ref. 11]. Again, the equivalent circuit shown in Fig. 2 provides a useful analogy.[35] Ordinarily, the sheath inductance can be ignored because the rate at which the current changes, dI/dt is relatively small. However, the sudden change in current, dI/dt large, created by the photodetachment process leads to an increased inductive impedance that limits the electron current. Thus, a resonant RLC circuit exists and current oscillations result from the sudden change in negative charge mobility. That these oscillations occur at a fre-

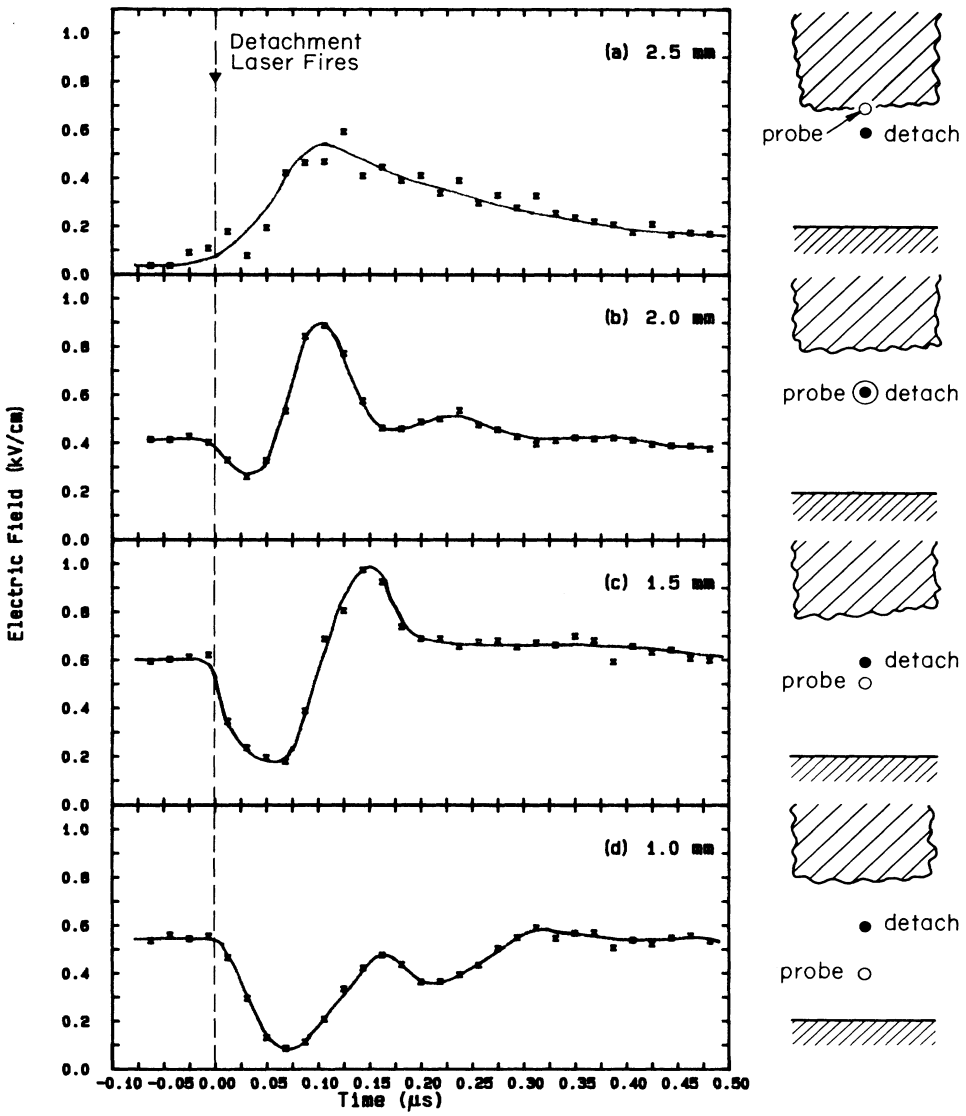

FIG. 4. Transient change in the local electric field resulting from photodetachment of BCl_3^- ions measured 2.5, 2.0, 1.5, and 1.0 mm below the upper electrode in (a)–(d), respectively. The magnitude of the field is deduced from the Stark-affected LIF spectra of BCl radicals near the photodetachment region (Ref. 9). Lead time refers to the time by which the photodetaching laser precedes the probe laser, which is triggered at $\omega t = 0.2\pi$. The drawings on the right schematically represent the relative positions of the probing and detaching laser beams with respect to each other, the electrode, and the plasma-sheath boundary. Note that the laser beam spot sizes are not drawn to scale.

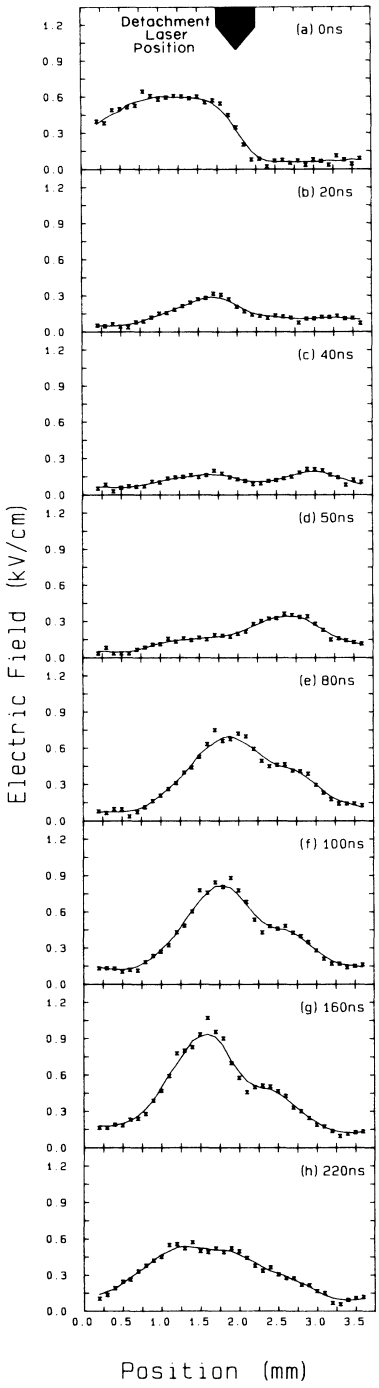

FIG. 5. Electric fields as a function of probe laser position for various times after firing the detachment laser, which is positioned 2.0 mm below the upper electrode. The probe laser is always fired at $\omega t = 0.2\pi$ while the detachment laser is fired at sequentially earlier times: 20, 40, 50, 80, 100, 160, and 220 ns in (a)—(h), respectively. The probe laser beam is scanned from 0 to 3.2 mm. The lines through the electric field measurements were generated by smoothing and interpolating the data shown by $\times$. The arrow at the top depicts where the detaching laser fires at $t=0$ ns; its width represents the detaching laser beam's FWHM intensity.

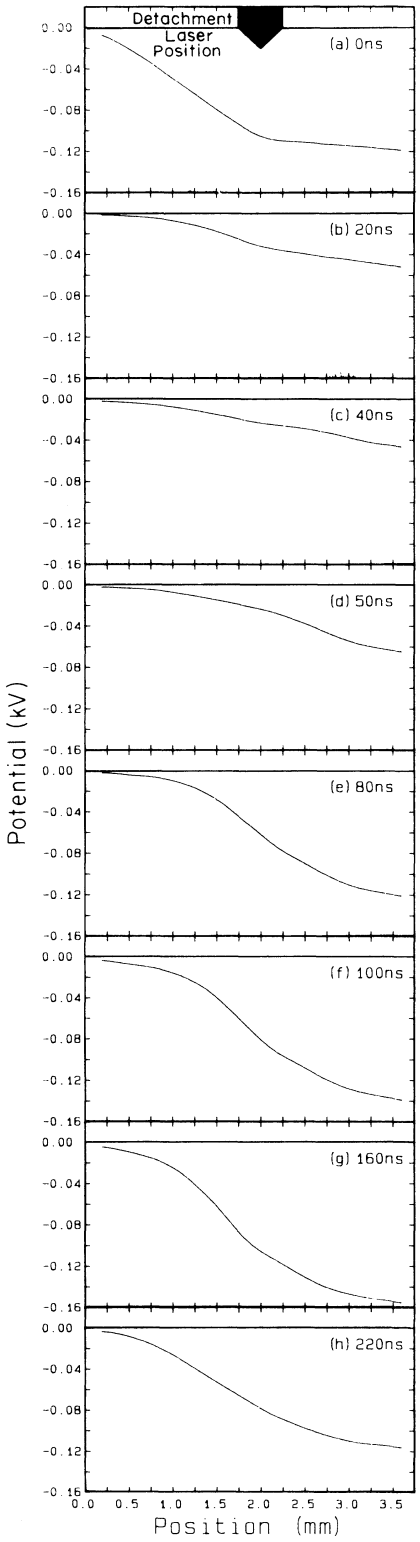

FIG. 6. Plasma potentials as a function of probe laser position for various times after firing the detachment laser (see caption to Fig. 4). The potentials are obtained by numerically integrating the fields from Fig. 4 and choosing the upper electrode (at 0 mm) to be at zero potential.

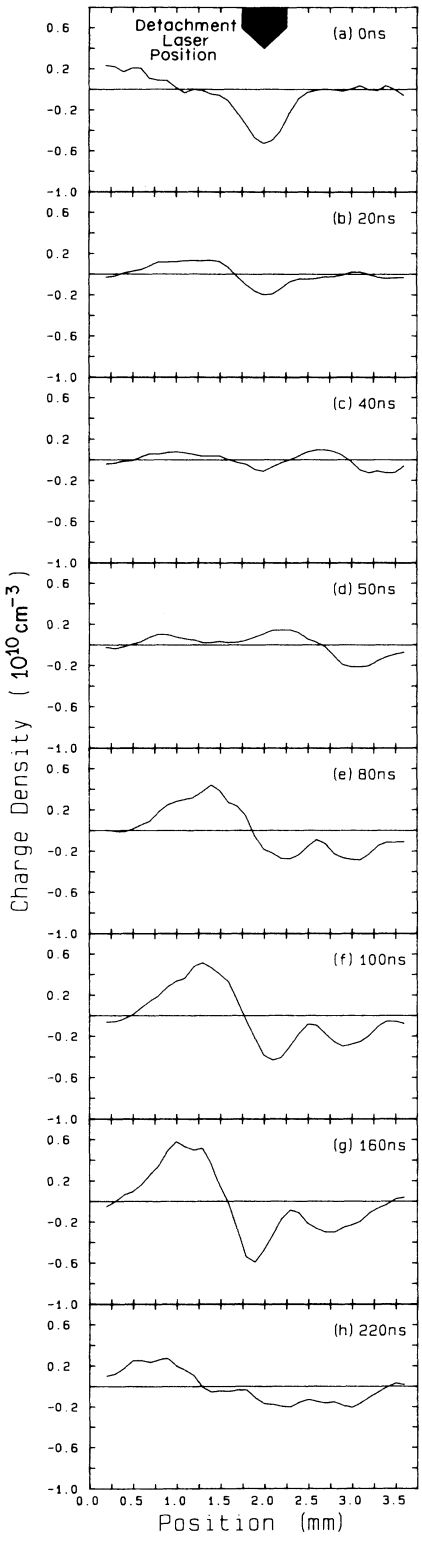

FIG. 7. Charge densities as a function of probe laser position for various times after firing the detachment laser (see caption to Fig. 4). The charge density curves were obtained by numerically differentiating the smoothed, interpolated field data in Fig. 4.

quency near the ion plasma frequency suggests that ion waves have been generated in response to the sudden change in negative charge mobility. Notice that in the plasma body [Fig. 4(a)], where the electron density is much smaller than the negative ion density, the oscillation appears to be over damped. This is consistent with the lack of ion acoustic mode development in an ion-ion plasma.[36] However, we do not feel that the oscillations lend themselves to simple interpretation given the absence of quasineutrality in the sheath and inhomogeneities in field and charge density. More detailed understanding must await the results of ongoing modeling efforts.[27]

(4) Relaxation of the field back to the predetachment level takes approximately 0.5 μsec, which is consistent with field-assisted ion drift into the detachment region: In a field of 300 V/cm, Cl^- ions drift approximately 0.05 cm in this time and would partially replenish the depleted anion density.[37] The apparent discrepancy between the relaxation times observed in Fig. 4 and the persistence of the optogalvanic signal for several cycles (Fig. 3) is attributed to a lack of sensitivity in the field measurements to total, absolute charge (or current) density. Until the charge density is fully restored to its predetachment level, deviations from the steady-state current waveform will be observed even though the local field is no longer noticeably changed.[38]

2. *Spatial variation of the field, potential, and charge density at several time delays*

Additional insight into the plasma response to photodetachment can be gained by examining the time evolution of the spatially-resolved plasma electric field, potential, and net charge density (Figs. 5, 6, and 7, respectively). These data are also shown as color contour plots in Figs. 8, 9, and 10, respectively.

The detachment laser beam position is fixed 2 mm below the upper electrode (arrows in Figs. 5–7) and the laser is fired at various times before the probe laser, which is fired at $\omega t = 0.2\pi$, The timing is done in this fashion because the initial plasma field is relatively time independent for 0.5 μs before 0.2π but not afterward.[11] To map out the field spatially, the probe laser beam is scanned from 0 to 3.6 mm away from the electrode.

Before photodetachment, the field exhibits a maximum near the plasma-sheath boundary [Figs. 5(a) and (8)] as a result of the different electron to negative ion concentration ratios on either side of the boundary:[11]

$$\left[\frac{n_e}{n_-}\right]_{\text{sheath}} > \left[\frac{n_e}{n_-}\right]_{\text{plasma}} .$$

This condition leads to a double layer with net positive charge on the electrode side of the boundary and net negative charge on the plasma side of the boundary [Figs. 2, 7(a), and 10].

Consistent with the temporal dependence displayed in Fig. 4, the local field initially decreases on the sheath side and increases on the plasma side of the boundary [Figs. 5(b) and 8]. The loss of negative charge causes the plasma potential to "float up" toward the anode potential [Figs. 6(b) and 9]. The penetration of the field into the plasma draws out additional negative charge and, in the process,

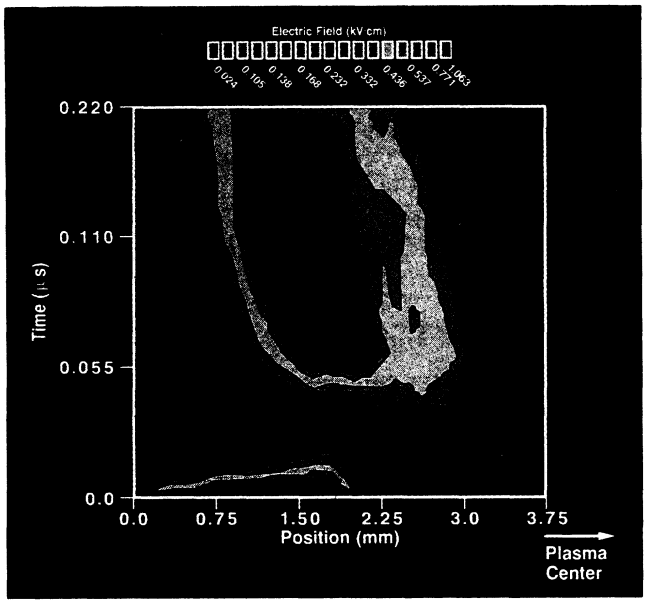

FIG. 8. Color contour plot of sheath electric fields in 50 kHz discharge through BCl_3 after photodetachment ($t=0$) of electrons from BCl_3^-. The position of the electrode is at 0 mm and the plasma center (not shown) is at 8.0 mm. The color scale is shown at the bottom. The plot is generated by linearly interpolating the data displayed in Fig. 5.

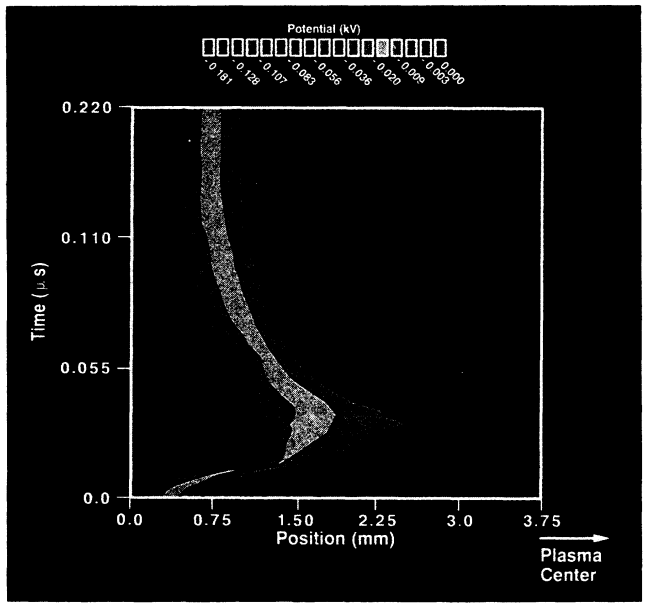

FIG. 9. Color contour plot of sheath potential in 50 kHz discharge through BCl_3 after photodetachment ($t=0$) of electrons from BCl_3^-. The position of the electrode is at 0 mm and the plasma center (not shown) is at 8.0 mm. The color scale is shown at the bottom. The plot is generated by linearly interpolating the data displayed in Fig. 6.

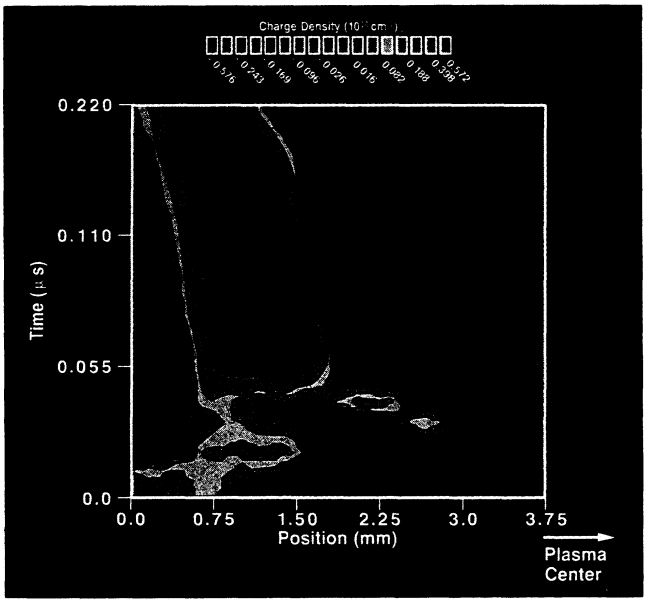

FIG. 10. Color contour plot of sheath charge density in 50 kHz discharge through BCl_3 after photodetachment ($t=0$) of electrons from BCl_3^-. The position of the electrode is at 0 mm and the plasma center (not shown) is at 8.0 mm. The color scale is shown at the bottom. The plot is generated by linearly interpolating the data displayed in Fig. 7.

two double layers form at $t\sim 40$ ns [Figs. 5(c), 7(c), and 10] which later merge into a single double layer at $t\sim 50$ ns. Subsequently (50—100 ns), the motion of net charge density ceases and the potential drop across the sheath increases (the plasma becomes more negative) [Figs. 6(f), 7(f), 9, and 10]. In terms of the equivalent circuit analogy discussed in Sec. III (Fig. 2), the inductive impedance increases as a result of the momentary increase in current and the sheath electric field increases as the current decreases.

By $t\sim 100$ ns, a single, large double layer has reformed, which persists as the potential slowly relaxes back to its initial level [Figs. 5(e)—5(h), 6(e)—6(h), 8, and 9]. During most of this time, the net charge density exhibits two minima [Figs. 7(e)—7(g) and 10].

IV. SUMMARY

In summary, we have demonstrated two methods for detecting photodetachment of electrons from negative ions in rf discharges. The first, an *ex situ* method, entails synchronization of the laser with the rf field driving the plasma. In this fashion, the full time dependence of the optogalvanic signal produced as a result of photodetachment in a BCl_3 plasma is recovered from the total discharge current waveform, The second, an *in situ* method, utilizes two lasers, one to photodetach and the other to excite Stark-mixed energy levels to deduce changes in the local electric field. Because of the *in situ* nature of the latter technique, it provides detailed information on not only the time dependence of the plasma response but also the spatial dependence. Therefore,

changes in plasma potential and charge density are determined directly.

The primary effect of photodetachment on the discharge is an initial increase in both plasma potential and sheath thickness followed by oscillations at a frequency of 6—7 MHz in both the local potential and the net current. A simple equivalent circuit description of the sheath is used to account qualitatively for most of the observations: The detachment laser pulse acts as a momentary short circuit of the sheath resistance by converting relatively immobile negative ions into mobile electrons. The resultant increase in current is impeded inductively and the field and current oscillate briefly.

The results presented here constitute stringent tests for kinetic and fluid model descriptions of photodetachment in discharges through strongly attaching gases. A more quantitative understanding of the optogalvanic effect and the kinetic balance responsible for sustaining the discharge will result upon the passing of these tests.

Finally, although our studies have been restricted to photodetachment of negative ions, the methods presented here require only that the mobility of the charge carriers change after the absorption of radiation (free electrons versus negative ions in this instance), and should therefore be equally well suited to the study of optogalvanic effects produced by a change in the ionization balance (see Refs. 39, 40, 41, and references therein) or a direct change in mobility.[42]

ACKNOWLEDGMENTS

We are grateful for stimulating discussions with V. M. Donnelly, D. B. Graves, T. Intratour, and L. C. Pitchford. The suggestion by T. Graedel to use color contour plots and their production by M. Harrison are gratefully acknowledged.

[1]J. Taillet, C. R. Acad. Sci. Paris **269**, 52 (1969).
[2]M. Bacal, G. W. Hamilton, A. M. Bruneteau, H. J. Doucet, and J. Taillet, Rev. Sci. Instrum. **50**, 719 (1979).
[3]M. Pealat, J-P. E. Taran, M. Bacal, and F. Hillion, J. Chem. Phys. **82**, 4943 (1985).
[4]C. R. Webster, and C. T. Rettner, Laser Focus **19(2)**, 41 (1983).
[5]C. R. Webster, I. S. McDermid, and C. T. Rettner, J. Chem. Phys. **78**, 646 (1983).
[6]R. Klein, R. P. McGinnis, and S. R. Leone, Chem. Phys. Lett. **100**, 475 (1983).
[7]K. E. Greenberg, G. A. Hebner, and J. T. Verdeyen, Appl. Phys. Lett. **44**, 299 (1984).
[8]C. A. Moore, G. P. Davis, and R. A. Gottscho, Phys. Rev. Lett. **52**, 538 (1984).
[9]M. L. Mandich, C. E. Gaebe, and R. A. Gottscho, J. Chem. Phys. **83**, 3349 (1985).
[10]J. Derouard and N. Sadeghi, Opt. Commun. **57**, 239 (1986).
[11]R. A. Gottscho and C. E. Gaebe, IEEE Trans. Plasma Science **14**, 92 (1986).
[12]On the time scale of the plasma response to the photodetachment laser pulse (~ 0.5 μs), the 50 kHz driving field is slow enough that the system may be viewed as a quasi-dc glow, albeit with density and potential profiles that are unlikely to occur in a dc glow.
[13]D. L. Flamm and V. M. Donnelly, Plasma Chem. Plasma Proc. **1**, 317 (1981).
[14]J. W. Coburn, Plasma Chem. Plasma Proc. **2**, 1 (1982).
[15]D. W. Hess, Solid State Technol. **24**, 189 (1981).
[16]D. W. Hess, Plasma Chem. Plasma Proc. **2**, 141 (1982).
[17]R. H. Burton, R. A. Gottscho, G. Smolinsky, *Dry Etching for Microelectronics*, edited by R. A. Powell (Elsevier, New York, 1984).
[18]L. A. D'Asaro, A. D. Butherus, J. V. Dilorenzo, D. E. Iglesias, and S. H. Wemple, *Proceedings of the 8th International Symposium on GaAs and Related Compounds*, Institute of Physics, Conf. Proc. No. 56 (Bristol, England, 1981), p. 267.
[19]R. A. Gottscho, G. Smolinsky, and R. H. Burton, J. Appl. Phys. **53**, 5908 (1982).
[20]R. A. Gottscho, G. P. Davis, and R. H. Burton, Plasma Chem. Plasma Proc. **3**, 193 (1983); J. Vac. Sci. Technol. A **1**, 622 (1983).
[21]R. A. Gottscho, R. H. Burton, D. L. Flamm, V. M. Donnelly, and G. P. Davis, J. Appl. Phys. **55**, 2707 (1984).
[22]R. A. Gottscho and M. L. Mandich, J. Vac. Sci. Technol. A **3**, 617 (1985).
[23]D. R. Lyons, A. L. Schawlow, and G. Y. Yan, Opt. Commun. **38**, 35 (1981).
[24]T. Suzuki, Opt. Commun. **38**, 364 (1981).
[25]R. Vasudev and R. N. Zare, J. Chem. Phys. **76**, 5267 (1982).
[26]J. Kramer, J. Appl. Phys. **60**, 3072 (1986).
[27]R. A. Gottscho (unpublished).
[28]D. B. Graves (private communication).
[29]G. L. Rogoff, J. M. Kramer, and R. B. Piejak, IEEE Trans. Plasma Sci. **14**, 103 (1986).
[30]Note that on the time scale in Fig. 3, the applied voltage does not change appreciably.
[31]R. N. Franklin, *Plasma Phenomena in Gas Discharges* (Clarendon, Oxford, 1976).
[32]J. S. Levine and F. W. Crawford, J. Plasma Phys. **23**, 223 (1979).
[33]N. Hershkowitz, Space Sci. Rev. **41**, 351 (1985).
[34]J. W. Gallagher, E. C. Beaty, J. Dutton, and L. C. Pitchford, J. Phys. Chem. Ref. Data **12**, 109 (1983).
[35]C. B. Zarowin, J. Electrochem. Soc. **130**, 1144 (1983).
[36]T. Intratour (private communication).
[37]Using an average charge exchange cross section for Cl^- in Cl_2 of 20 $Å^2$, [M. S. Huq, D. Scott, N. R. White, R. L. Champion, and L. D. Doverspike, J. Chem. Phys. **80**, 3651 (1984)] we estimate the high-field anion drift velocity, in cm/sec, at 0.3 Torr to be $3.8\times 10^3 E^{1/2}$, where E is in V/cm. Thus, in a 300 V/cm field, Cl^- drifts ~ 0.05 cm in 0.5 μsec.
[38]In other molecular systems, the same technique can be used with higher sensitivity [J. Derouard and N. Sadeghi, Opt. Comm. **57**, 239 (1986)] (~ 5 V/cm) and the apparent discrepancy noted here may not be present.
[39]J. Pfaff, M. H. Begemann, and R. J. Saykally, Mol. Phys. **52**, 541 (1984).
[40]D. K. Doughty and J. E. Lawler, Phys. Rev. A **28**, 773 (1983).
[41]E. F. Zalewski, R. A. Keller, and R. Engleman, Jr., J. Chem. Phys. **15**, 1015 (1979).
[42]R. Walkup, R. W. Dreyfus, and Ph. Avouris, Phys. Rev. Lett. **50**, 1846 (1983).

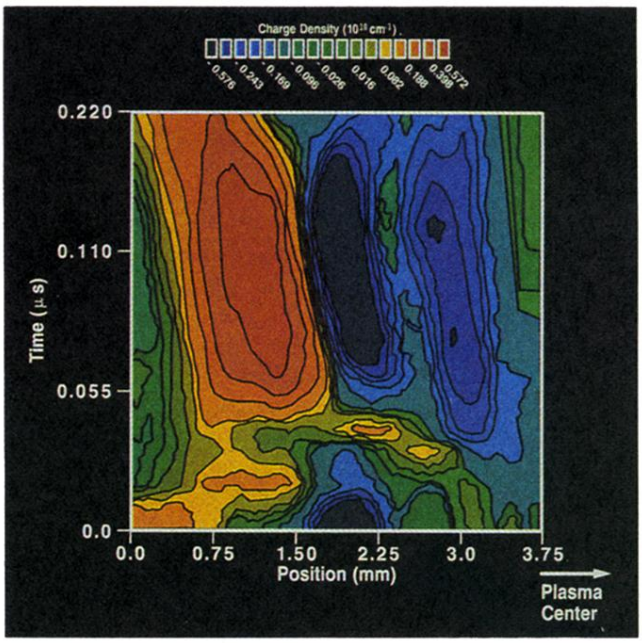

FIG. 10. Color contour plot of sheath charge density in 50 kHz discharge through BCl_3 after photodetachment ($t=0$) of electrons from BCl_3^-. The position of the electrode is at 0 mm and the plasma center (not shown) is at 8.0 mm. The color scale is shown at the bottom. The plot is generated by linearly interpolating the data displayed in Fig. 7.

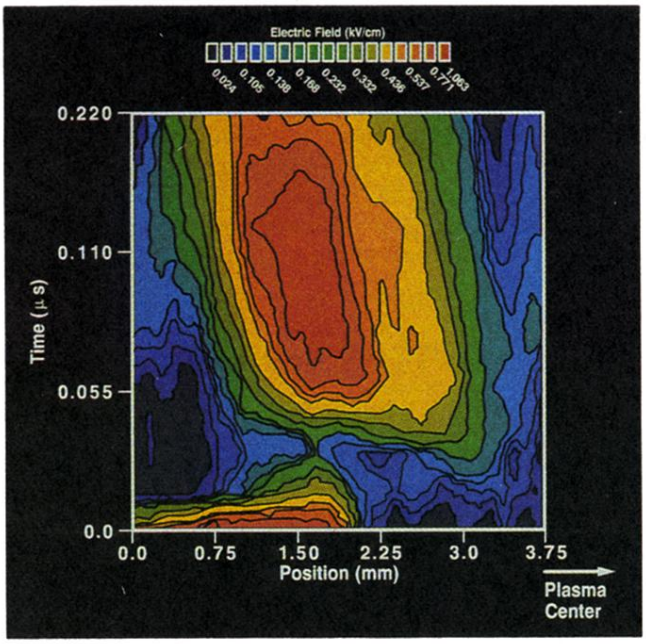

FIG. 8. Color contour plot of sheath electric fields in 50 kHz discharge through BCl_3 after photodetachment ($t=0$) of electrons from BCl_3^-. The position of the electrode is at 0 mm and the plasma center (not shown) is at 8.0 mm. The color scale is shown at the bottom. The plot is generated by linearly interpolating the data displayed in Fig. 5.

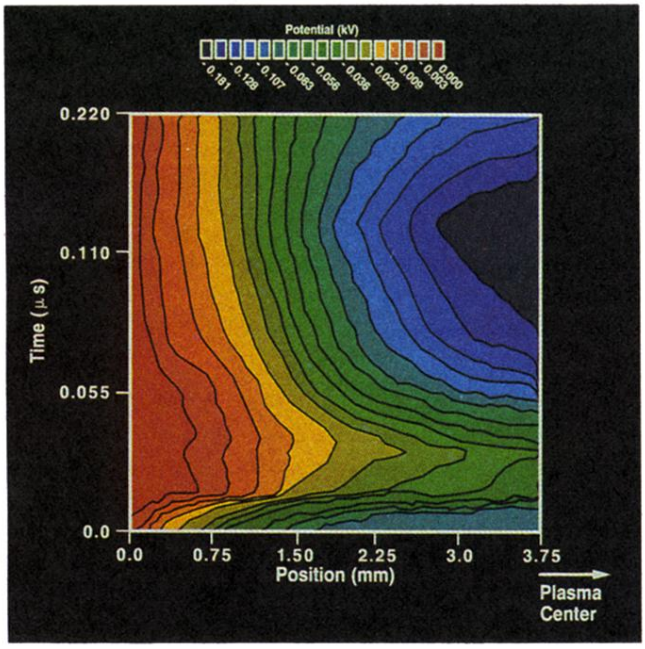

FIG. 9. Color contour plot of sheath potential in 50 kHz discharge through BCl_3 after photodetachment ($t=0$) of electrons from BCl_3^-. The position of the electrode is at 0 mm and the plasma center (not shown) is at 8.0 mm. The color scale is shown at the bottom. The plot is generated by linearly interpolating the data displayed in Fig. 6.